



1 **Dangerous degree forecast of soil and water loss on highway slopes in**
2 **mountainous areas using RUSLE model**

3 **Yue Li^{1,2}, Shi Qi^{*1,2}, Bin Liang^{1,2}, Junming Ma^{1,2}, Baihan Cheng^{1,2}, Cong Ma³, Yidan Qiu³,**
4 **and Qinyan Chen³**

5 ¹ Key Laboratory of State Forestry Administration on Soil and Water Conservation, Beijing
6 Forestry University, Beijing 100083, China

7 ² Beijing Engineering Research Center of Soil and Water Conservation, Beijing Forestry
8 University, Beijing 100083, China

9 ³ Yunnan Science Research Institute of Communication & Transportation, Kunming 650011,
10 China

11

12 **Abstract.** Many high and steep slopes have been formed by special topographic and geomorphic
13 types and mining activities during the construction of mountain expressways. Severe soil erosion
14 may occur under heavy rainfall conditions and pose a serious threat to road safety and the lives of
15 residents. Therefore, the prediction of soil and water loss on highway slopes is important for the
16 protection of infrastructure and human life. This work studies Xinhe Expressway, which is in the
17 southern edge of Yunnan Guizhou Plateau, as the research area. The revised universal soil loss
18 equation is selected as the prediction model of soil and water loss on slopes. Moreover, geographic
19 information system, remote sensing technology, field survey, runoff plot observation test, cluster
20 analysis, and cokriging are adopted. The partition of the prediction units of soil and water loss on
21 the expressway slope in the mountain area and the spatial distribution model of the linear highway
22 rainfall are studied. In view of the particularity of the expressway slope in the mountain area, the
23 model parameter factor is modified and the risk of soil and water loss along the mountain
24 expressway is simulated and predicted under 20-year and one-year rainfall return periods. The
25 results are as follows. (1) Considering natural watershed as the prediction unit of slope soil erosion
26 can represent the actual situation of soil and water loss of each slope. The spatial location of soil
27 erosion unit is realized, the accuracy of soil and water loss prediction results is improved, and the
28 convenience of data management and maintenance in the later stage is guaranteed. (2) Analysis of
29 the actual observation data show that the overall average absolute error of the monitoring area is
30 33.24 t·km⁻², the overall average relative error is 33.96%, and the overall root mean square error
31 is between 20.95 and 65.64, all of which are within acceptable limits. The Nash efficiency
32 coefficient is 0.67, thereby showing that the prediction accuracy of the model satisfies the
33 requirements. (3) Under the condition of one-year rainfall, we find through risk classification that
34 the percentage of prediction units with no risk of erosion is 78% and that with mild soil erosion
35 risk is 15.92%. Results show that soil erosion risk is low and thereby does not affect road traffic
36 safety. Under the 20-year rainfall condition, the percentage of units with high and extremely high
37 risk is 7.11%. In these areas, the risk of soil erosion is relatively large and mainly distributed on
38 K109+500–K110+500 and K133–K139+800 sections. Even if only part of the sediment is



39 deposited on the road, road safety will be affected. The prediction results can help adjust the
40 layout of water and soil conservation measures in these units. This study provides not only a
41 scientific basis for soil erosion prevention and control in mountain expressways but also a
42 reference for the application of water and soil loss prediction and soil conservation planning.

43

44 **Key words:** Soil and water loss; Highway slopes; Mountainous areas; RUSLE;
45 Dangerous degree forecast

46

47 1 Introduction

48

49 China has been gradually accelerating the construction of highways in recent years, thereby
50 improving the transportation network and driving rapid economic development. Especially with
51 the implementation of the western development strategy of the country, advanced requirements
52 have been proposed for the construction of expressways, which focuses on gradually connecting
53 the coastal plains and the inland mountains (Tan and Wang 2004; Song et al., 2008; Jia and Guo
54 2008; Wang and Gao 2015). Many unstable high and steep slopes, such as natural, excavation, and
55 fill slopes, are inevitably formed by the considerable filling and deep digging along expressways
56 in mountain areas.

57 The slope is the most fragile part of an expressway in a mountain area. During the rainy season,
58 soil erosion is easily caused by rainwash and leads to a worrisome extent of damage (Figure 2).
59 According to statistics, along with the development of highway construction in China, slope areas
60 reach 200–300 million m² each year. In the next 20–30 years, expressways in China will measure
61 more than 40 thousand km. For every kilometer of a highway, the corresponding bare slope area
62 formed measures 50–70 thousand m². The annual amount of soil erosion is 9000 g/m², which
63 causes 450 t of soil loss every year (Chen 2010). Compared with forestlands and farmlands, the
64 soil and water loss on subgrade slopes is special. Forestlands and farmlands are generally formed
65 after years of evolution and belong to the native landscape. Most slopes are gentle and stable.
66 Traditional soil and water conservation research focuses on slopes with 20% grade or below, but
67 the highway subgrade slope of steep slopes is generally greater than 30% (Zhou 2010). Soil
68 erosion on subgrade side slopes affect not only soil and water loss along the highway but also safe
69 road operation (Gong and Yang 2016; Jiang et al., 2017). Therefore, the study of soil erosion on
70 the side slopes of mountain expressways is significant for controlling soil erosion, improving the
71 ecological environment of the expressway, and realizing sustainable land utilization (Wang et al.,
72 2005; Yang and Wang 2006).

73 For a long time, the use of revised universal soil loss equation (RUSLE) model as a predictive
74 tool for the quantitative estimation of soil erosion has been maturing. The range of application of



75 these models involves nearly every aspect of soil erosion (Wischmerie and Smith 1965; Renard et
76 al., 1997; Millward and Mersey 1999; Shi et al., 2004; Bosco et al., 2015; Stanchi et al., 2014;
77 Fenta et al., 2016; Molla and Sisheber 2017; Zeng et al., 2017; Wang et al, 2017). In addition,
78 many scholars have explored the process of using the RUSLE model. They combined research
79 objects to correct the parameter values in this model, thus improving simulation accuracy. Tresch
80 S et al. (1995) believed that the topographical factor *LS* is one of the main factors for soil erosion
81 modeling within the RUSLE environment. Various S-factors exist for the most used soil erosion
82 modeling environment and significantly influence calculated erosion values. All existing S-factors
83 are only derived from gentle slope inclinations (up to 32%). Many cultivated areas, particularly in
84 Switzerland, are steeper than this critical value. Eighteen plot measurements on transects along
85 slopes ranging from 20%–90% in steepness were used in this study to qualitatively assess the most
86 suitable S-factors for steep subalpine slopes. Results showed that a first selection of an S-factor for
87 slopes above the critical 25% steepness is possible (Tresch et al., 1995). Rick D (2001) found that
88 using universal soil loss equation (USLE) and RUSLE soil erosion models at regional landscape
89 scales is limited by the difficulty of obtaining an LS-factor grid, which is suitable for use in
90 geographic information system (GIS) applications. Therefore, he described the additions and
91 modifications applied to the previous arc macro language (AML) code to produce a RUSLE-based
92 version of the *LS* factor grid. These alterations included replacing the USLE algorithms with their
93 RUSLE counterparts and redefining assumptions on slope characteristics. Finally, in areas of
94 western USA where the models were tested, the RUSLE-based AML program produced *LS* values
95 that were roughly comparable to those listed in the RUSLE Handbook guidelines (Rick et al.,
96 2001). The study of Silburn DM (2011) showed that the method used to estimate K from soil
97 properties (derived from cultivated soils) provides a reasonable estimate of K for the main duplex
98 soils at the study site as long as the correction for undisturbed soil is used to derive K from the
99 measured data and applying K to the USLE model. However, methods used to fit the parameters
100 affected the results, and minimizing the sum of the squares of errors in the soil losses provided
101 better results than fitting an exponential equation (Silburn 2011). Yang (2014) found that the C-
102 factor value can be determined as a function of fractional bare soil and ground cover derived from
103 MODIS data at regional or catchment scales. The method offers a meaningful estimate of the C-
104 factor, thus indicating ground cover impact on soil loss and erosion hazard areas. The method is
105 better than the commonly used models, which are based only on green vegetation (e.g.,
106 normalized difference vegetation index, NDVI). Thus, the study provided an appropriate approach
107 to estimating the C-factor in hillslope erosion modeling in New South Wales, Australia, using
108 emerging fractional vegetation cover products. This approach is a simple and effective way to map
109 the spatial and temporal distribution of the RUSLE cover factor and hillslope erosion hazard in



110 large areas. The methods and results described in the current article are valuable for understanding
111 the spatial and temporal dynamics of hillslope erosion and ground cover (Yang 2014).
112 According to a study by Kinnell PIA (2014), runoff production, which is spatially uniform, is
113 often inappropriate under natural conditions, where infiltration is spatially variable. The use of an
114 upslope slope length that varies with the ratio of the upslope runoff coefficient to the runoff
115 coefficient for the area down to the downslope boundary of the segment in modifications of the
116 RUSLE approach produces only minor variations in soil loss compared with those predicted using
117 the standard RUSLE approach when the runoff is spatially variable and the number of segments
118 increases. On the contrary, the USLE-M approach provides predictions of soil loss that are
119 influenced strongly by runoff when runoff varies in space and time. Therefore, an increase in the
120 runoff through a segment produces an increase in soil loss, whereas a decrease in the runoff
121 through a segment or cell produces a decrease in soil loss (Kinnell 2014).

122 However, these studies are mainly limited to sloping fields. The research on soil erosion in
123 highway slopes is weak. Subgrade slope is a major part of soil erosion in construction and
124 operation periods. Therefore, the soil erosion caused by this slope should be predicted. However,
125 the accumulation degree of soil and water loss in highways cannot satisfy the requirements of
126 model development. To date, no mature model of soil erosion in highways is available. The
127 situation in various regions in China show that certain researchers have improved the RUSLE
128 model and studied soil erosion that occurs in certain areas. Yang (2001) investigated the behavior
129 of soil erosion on the slope of railway embankments during construction by comparing artificial
130 and natural rainfalls on the special Qinhuangdao–Shenyang line of passenger trains. The results
131 showed that the main type of soil erosion in the study area was gully erosion, which caused more
132 soil erosion than surface erosion did, and the principal factor causing soil erosion on the slope was
133 the amount of precipitation and the width of the embankment (Yang et al., 2001). Wang (2005)
134 established several experimental standardized spots for soil loss collection on the side slopes of
135 the Xiaogan–Xiang fan freeway under construction and installed an on-the-spot auto-recorder of
136 rainfall. The data collected were used for the revision of the main parameters R (rainfall and
137 runoff) and K (erodibility of soil) of the USLE, which is widely applied to forecast soil loss
138 quantity in plowlands and predict the soil loss quantities of different types of soil on side slopes
139 disturbed by engineering treatment. The study concluded that the optimal parameter representation
140 for R and K (Wang et al., 2005).

141 According to studies at home and abroad, the study of soil and water loss in highways have the
142 following problems. (1) In using the RUSLE model, most of the research on the C and P factors is
143 conducted by referring to previous research results and data accuracy is often defective. (2) Most
144 studies on rainfall erosivity (R) factors are still limited to sloping fields (Wang and Zhang 1995;



145 Shamshad et al., 2008; Angulomartínez and Beguería 2009; Panos et al., 2015; Lin et al., 2017),
146 and few studies have been carried out on the rainfall erosivity factors of expressway slopes in
147 mountain areas. (3) Slope soils in highways differ from the broad sense of arable soil; moreover,
148 the slopes themselves are also varied. Thus, the soil loss of different types of subgrade slopes is
149 difficult to accurately predict using the traditional K factor calculation method.

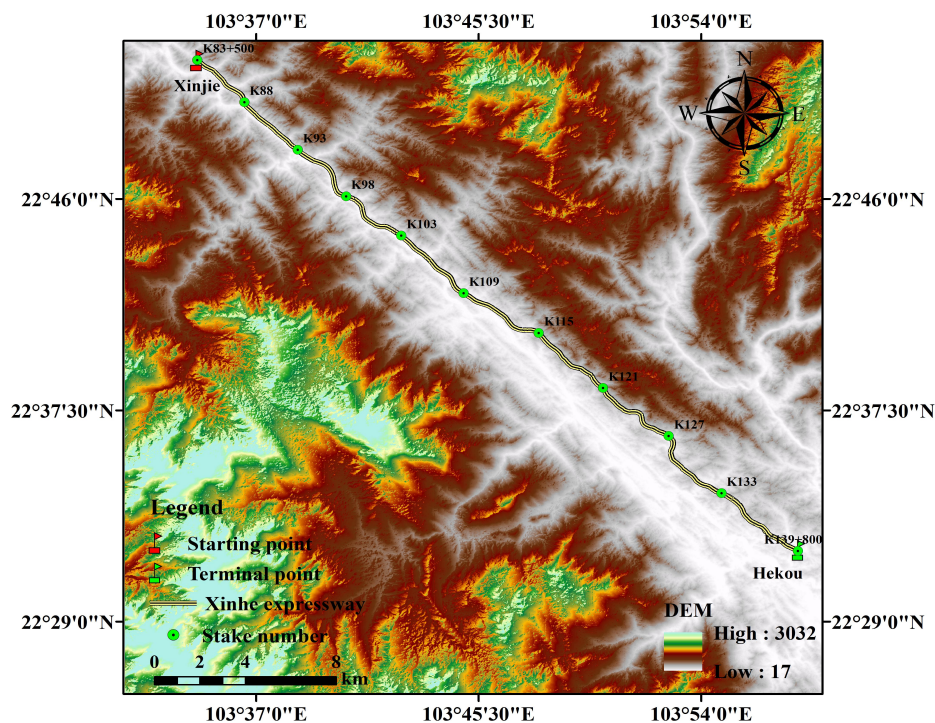
150 Therefore, the RUSLE equation is selected as the prediction model for soil and water loss on
151 slopes with GIS technology as support in view of the characteristics of soil and water loss in
152 mountain expressways. The soil erodibility factor (K), slope length factor (LS), and soil and water
153 conservation measure factor (P) are revised to improve the method of dividing slope units. In
154 determining the predictive parameters of the model, the R factor is obtained by spatial
155 interpolation, thus resolving the shortage of rainfall data in mountains areas and addressing the
156 difficulty of representing the rainfall data of the entire expressway with data from a single
157 meteorological station and the uneven spatial distribution and strong heterogeneity of rainfall in
158 mountain areas. A suitable prediction model of soil and water loss is established, the parameters of
159 the model are revised, and the risk of soil and water loss under different rainfall scenarios is
160 simulated and predicted. This study scientifically predicts the amount of soil erosion caused by
161 highway construction in mountain areas not only for the rational layout of facilities, which reduces
162 damage to the original topography and effectively prevents and controls new soil erosion, but also
163 provides scientific and technical basis and reference methods. Meanwhile, the safe operation of
164 highways and the virtuous cycle of the ecological environment should be ensured to promote the
165 sustainable development of the local economy.

166 2 Study area

167 Xinhe Expressway is in the southern margin of the Yunnan–Guizhou Plateau, which is in southeast
168 Yunnan Province, Honghe Prefecture, and Hekou County. This highway was the first in Yunnan to
169 cross the border, thereby becoming an important communication channel between China and
170 Vietnam and obtaining important strategic and economic value. The highway is located at
171 longitude $103^{\circ} 33' 45''$ – $103^{\circ} 58' 32''$ and latitude $22^{\circ} 31' 19''$ – $22^{\circ} 51' 48''$. The expressway
172 stretches roughly from northwest to southeast, and the total length is 56.30 km. The climate type
173 belongs to subtropical mountain, seasonal monsoon forest, and humid heat climate categories.
174 Between May and mid-October, the area experiences the wet season, which is characterized by
175 abundant rainfall, concentrated precipitation, and increased rain at night. During the rest of the
176 year, the area undergoes dry season. The starting point of Xinhe Expressway is in Hekou County,
177 New Street (pile number K83+500) at an altitude of 296 m. The stop point is in the estuary of
178 Areca Village (pile number K139+800) at an altitude of 95 m. The terminal is across the river
179 from the old street of Vietnam. The mountains along both sides are 200–380 m above sea level
180 (Figure 1). The topography of the hilly area in the northern part of Xinhe Expressway is
181 complicated. The slopes on both sides rise and fall, and most of the valleys constitute “V”- and
182 “U”- shaped sections. The natural slopes on both sides are mostly below 30° . The southern part of



183 the highway has a relatively flat terrain and a gentle slope. The slope of most of the hills on both
184 sides is less than 15°, and the overall height difference is smaller than 100 m. The vegetation in
185 the southern part of the Xinhe Expressway includes tropical rainforests and tropical monsoon
186 forests. Meanwhile, the vegetation in the northern part of China is classified as a south subtropical
187 monsoon evergreen broad-leaved forest. In recent years, the original vegetation in this area has
188 been reclaimed as farmland and is now planted with rubber, banana, pineapple, and pomegranate,
189 which are sporadic tropical rainforest survivors. The project area along the Xinhe Expressway is
190 an economic forest belt with a single vegetation type and mainly has rubber, forest, and other
191 economic trees. The soil types along the highway are rich and mainly red, leached cinnamon, gray
192 forest, and gray cinnamon soils.



193
194

Figure 1. Overview of the study region



Figure 2. Soil erosion produced by rainwash on slope

3 Materials and method

3.1 Data sources

3.1.1 Meteorological data

Rainfall data from 2014 were obtained from Hekou Yao Autonomous County, Pingbian Miao Autonomous County, Jinping Miao Yao Autonomous County, and the meteorological department of Mengzi. The rainfall data type was in 5 min format. Meanwhile, two automatic weather stations were set up along Xinhe Expressway to gather weather data during the 2014 experiment. Meteorological data acquired from the China Meteorological Data Network covered the period of 1959–2015 (<http://data.cma.cn/site/index.html>).

3.1.2 Soil data

Soil type data were provided by Yunnan Traffic Planning and Design Institute. Soil texture and organic matter data were obtained by field surveys, data sampling, and processing methods. Soil samples were collected from every 1 km of the artificial and natural slopes on both sides of the highway. The five mixed soil samples of one slope were obtained using the “S”-shaped sampling method. Then, the quartering method was adopted, and 1/2 soil samples from the mixed soil samples were brought to the laboratory for analysis. Finally, 186 soil samples were obtained. After the soil samples were dried and sieved, we measured the soil texture and organic carbon content through specific gravity speed measurement and potassium dichromate external heating, respectively.



3.1.3 Topographic data

The topographic map and design drawings of Xinhe Expressway were provided by the Traffic Planning and Design Institute of Yunnan Province. The 1:2000 scale of the topographic map coordinate system was based on the 2000 GeKaiMeng urban coordinate system, elevation system for the 1985 national height datum, and the format for the CAD map DWG format.

2.1.4 Image data

The remote sensing images used in this study were derived from 8m hyperspectral images produced by GF-1 satellite (<http://www.rscloudmart.com/>).

2.2 Predicting model selection

The RUSLE equation was used to predict soil and water loss on the side slopes of Xinhe Expressway. The RUSLE equation considers natural and anthropogenic factors that cause soil erosion to produce comprehensive results. Various parameters are easy to calculate, and the calculation method is relatively mature. The RUSLE model is suitable for soil erosion prediction in areas where the physical model is not needed. See Formula (1) (Renard et al., 1997).

$$A = R \cdot K \cdot L \cdot S \cdot C \cdot P, \quad (1)$$

where A is the average soil loss per unit area by erosion (t/hm^2), R is the rainfall erosivity factor ($MJ \cdot mm / (hm^2 \cdot h)$), K is the soil erodibility factor ($t \cdot hm^2 \cdot h / (hm^2 \cdot MJ \cdot mm)$), L is the slope length factor, S is the steepness factor, C is the cover and management practice factor, and P is the conservation support practice factor. The values of L , S , C , and P are dimensionless.

4 Results and analysis

4.1 Prediction unit division and implementation

Geological structures and rock and soil categories are complex because of considerable changes in topography and physiognomy. The forms of slopes also vary. In general, according to the relationship between slope and engineering, slopes can be natural or artificial. Artificial slope formations can be subdivided into slope embankments and cutting slopes. This study used ArcGIS software to convert the topographic map of the highway design into a vectorization file because the artificial and natural slopes of watershed catchments are the main components of soil erosion prediction. The natural and artificial slope catchment watershed was divided into uniform prediction units on the basis of the extracted graphical units of the artificial natural slope catchments and according to the differences in aspect, slope, land use, and water conservation measures, such as property. The aspect, slope, land use, water conservation measures, and other attributes of each prediction unit were consistent. A schematic of the division process is shown in Figure 3.

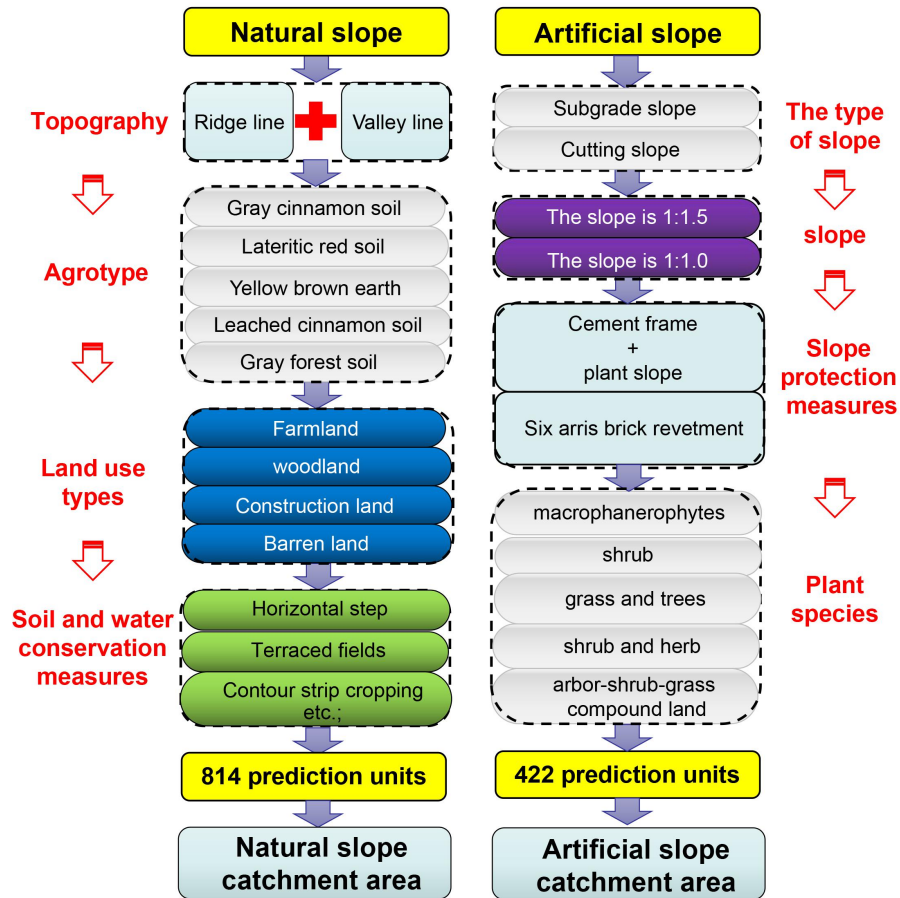


Figure 3. Prediction unit division

4.1.1 Natural slope catchment area

The catchment unit of the slope was constructed using the structural plane tools of ArcGIS platform combined with ridge and valley lines and artificial slope and highway boundaries. After the completion of the catchment unit, the slope was divided according to soil type data (Table 1). After the division and overlaying of the remote sensing image map, the land use types and soil and water conservation measures were considered indicators through visual interpretation and field survey results in further classifying the confluence units. Finally, the partition units were amended using the vegetation coverage data obtained along Xinhe Expressway. A total of 814 natural slope catchment prediction units were divided.



Table 1. Distribution of soil types along Xinde Expressway

A section of a expressway	Soil type
K83+500~K84+900	latosolic red soil
K85+200~K93+200	leached cinnamon soil
K93+200~K95+900	gray forest soil
K96+900~K97+800	gray cinnamon soil
K97+800~K100+500	leached cinnamon soil
K100+500~K101+100	gray cinnamon soil
K101+100~K104	leached cinnamon soil
K104~K109+100	gray cinnamon soil
K109+100~K139	leached cinnamon soil

The artificial slope was divided into roadbed and cutting slopes according to the design of Xinde Expressway into 1:1.5 and 1:1.0 slopes. After the preliminary division, the slope measurements, data design, and field survey results were used as bases for the subsequent detailed division of the artificial slope into cement frame protection and six arris brick revetments. The study of McCool stated that slope length varies within the 10 m range and has little effect on the results (McCool et al., 1997). The specifications of each frame in the cement frame protection along Xinde Expressway are the same. The horizontal projection length of the cement frame is the slope length value of the artificial slope. Therefore, the slope length of the artificial slope of each frame of the cement revetment was considered the same and with a value of 0. According to the investigation, the vegetation coverage of artificial slopes with different plant species is greatly different. To achieve an accurate prediction of unit division and improve prediction accuracy, the artificial slopes should be continuously classified according to the plant species. A total of 422 artificial slope prediction units were thus obtained. The main process is shown in Figure 3. Then, the data about the 1236 slope prediction units were edited using GIS. The results are shown in Figure 4.

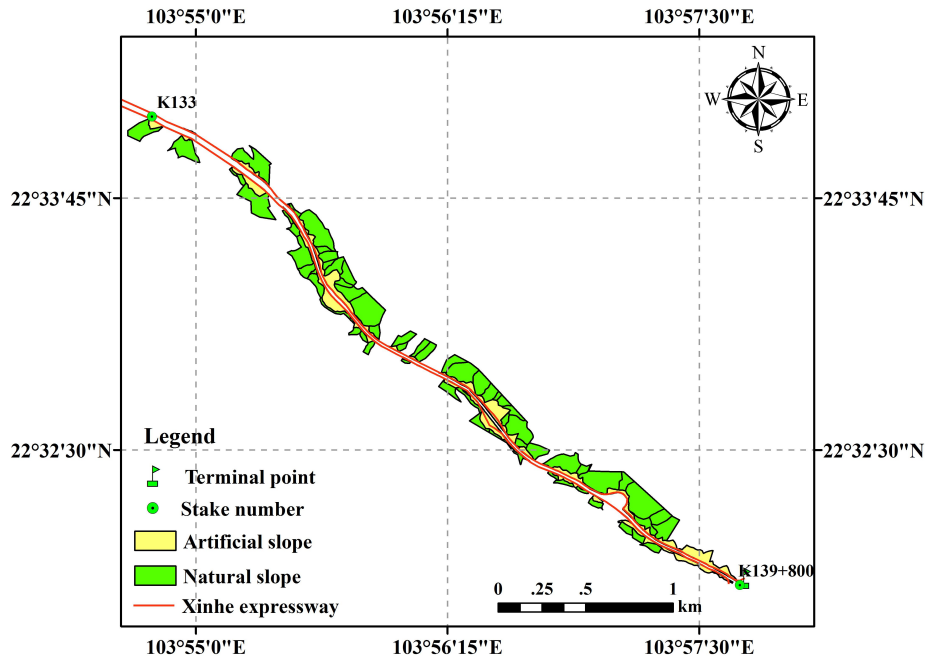


Figure 4. Division results of prediction units (K133–K139)

4.2 Determination of conventional parameter factor values of RUSLE model

4.2.1 Rainfall erosivity factor (R)

The formula of the R value of rainfall erosivity was adopted. The R value was calculated using 30 min rainfall intensity as a measure, as shown by Formulas (2) and (3).

$$R = 1.70 \cdot (P \cdot I_{30} / 100) - 0.136 \quad (I_{30} < 10 \text{ mm/h}), \quad (2)$$

$$R = 2.35 \cdot (P \cdot I_{30} / 100) - 0.523 \quad (I_{30} \geq 10 \text{ mm/h}), \quad (3)$$

where R is the rainfall erosivity, P is the sub-rainfall, and I_{30} is the maximum 30 min rainfall intensity.

The rainfall data were obtained from stationary ground meteorological stations. Thus, using data from a single meteorological station to represent the rainfall data of a linear mountain expressway was difficult. The P and I_{30} values along the highway were obtained by interpolation calculations. The data included those derived from rainfall and 30 min rainfall data from four meteorological stations in Hekou Yao Autonomous County, Pingbian Miao Autonomous County, Jinping Miao Yao Autonomous County, and Mengzi City, and data from two automatic weather stations along the highway (Chen 2016). Then, the cross-validation method was used to evaluate the accuracy of the interpolation results. The selection criteria were standard root mean square error and the mean standard error. Detailed results are shown in Table 2. This paper shows only



the interpolated results of secondary rainfall of two rainfall and 30 min rainfall intensity data, as shown in Figures 5–8.

Table 2. Interpolation error of P and I_{30} values

The time of the second rainfall	P		I_{30}	
	RMSS	MS	RMSS	MS
2014.06.05	1.02	-0.02	1.06	-0.05
2014.06.07	1.04	-0.02	1.01	0.02
2014.06.17	1.09	0.03	1.11	0.06
2014.06.28	1.11	0.07	1.05	-0.03
2014.07.01	1.10	0.04	1.06	-0.04
2014.07.13	1.03	-0.02	1.01	0.02
2014.07.20	1.01	0.01	1.05	0.02
2014.08.02	1.03	0.03	0.94	0.02
2014.08.12	1.05	-0.03	1.10	0.03
2014.08.26	1.03	0.01	0.97	0.03
2014.08.29	1.09	-0.02	1.03	-0.02
2014.09.02	1.07	0.03	1.05	0.02
2014.09.04	0.96	-0.02	0.97	-0.02
2014.09.17	1.07	-0.03	1.09	-0.03
2014.09.20	0.98	0.05	1.03	0.02
2014.10.05	1.02	0.03	1.04	0.03

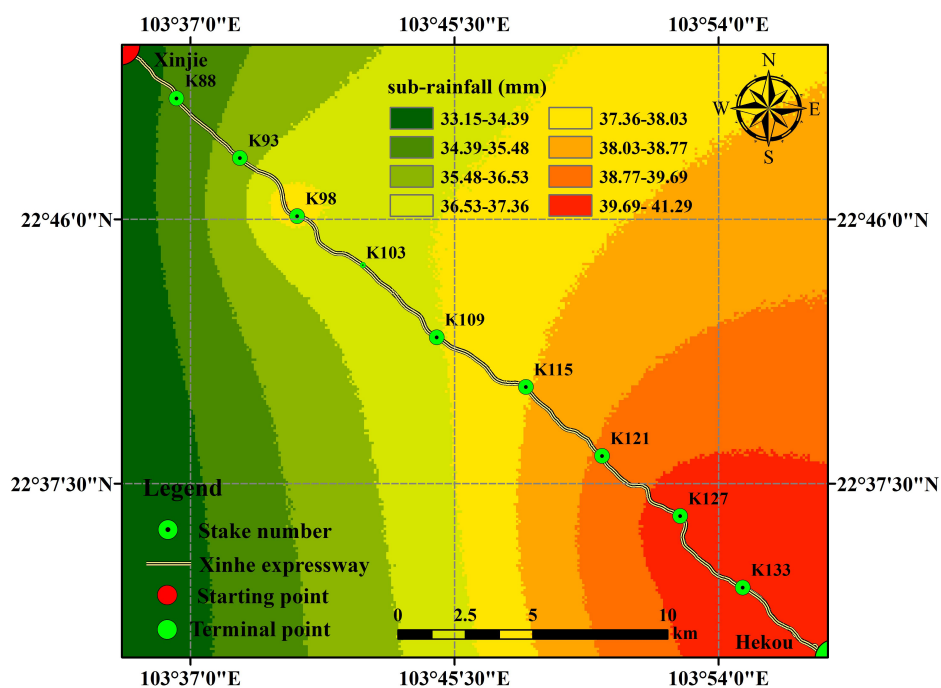


Figure 5. Interpolation results of secondary rainfall for June 5, 2014

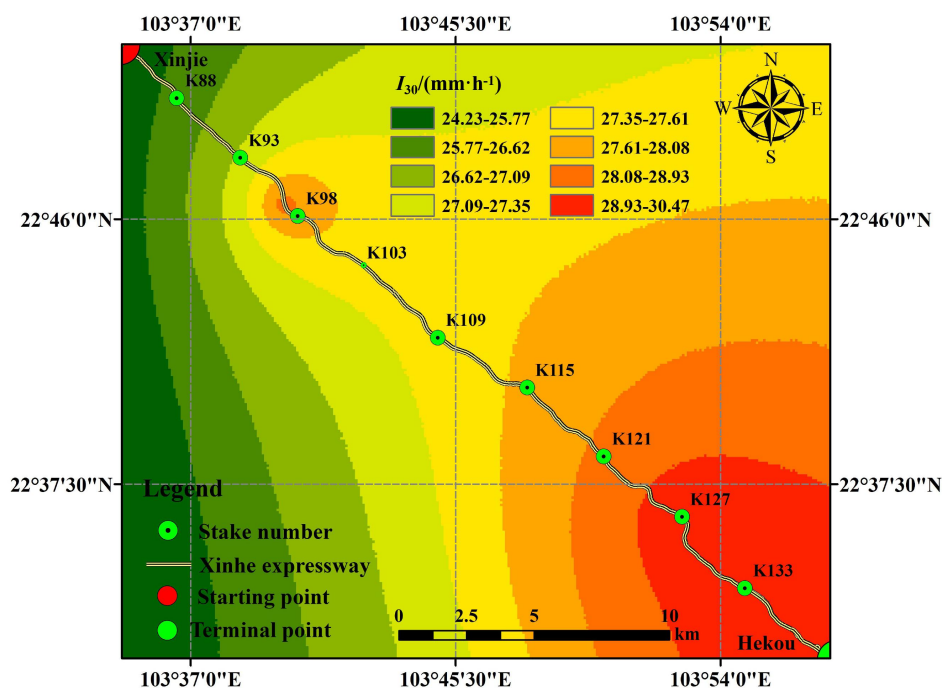


Figure 6. Interpolation results of I_{30} for June 5, 2014

The secondary rainfall data of 16 rainfall instances along the Xinhe Expressway were obtained by interpolation because the internal rainfall and rainfall intensity of a single prediction unit were the same. Therefore, the R value was calculated using the average rainfall and rainfall intensity of the unit. Only the spatial distribution map of the rainfall erosivity factors in certain sections (June 5, 2014) is shown in Figure 7 due to space constraints.

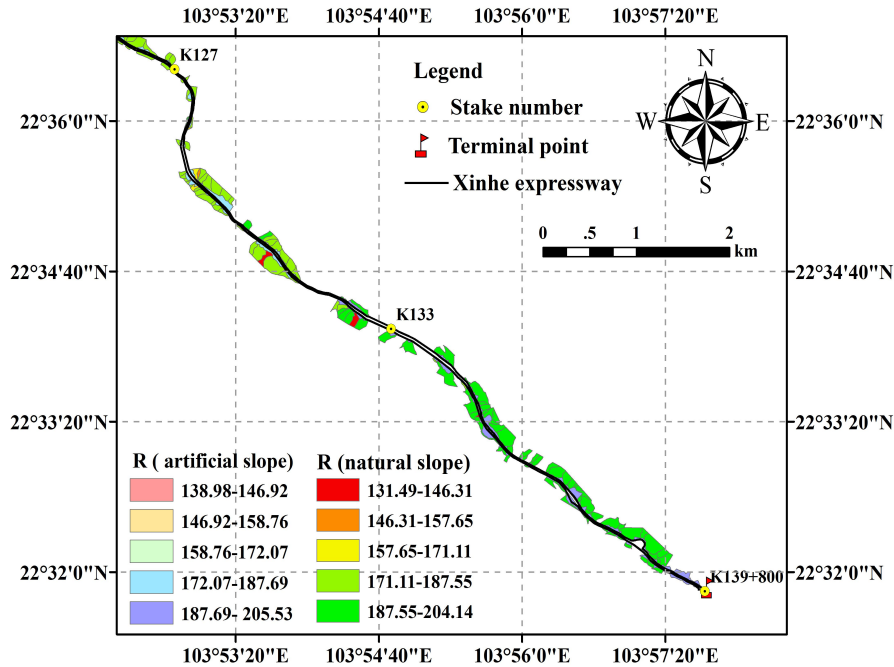


Figure 7. Spatial distribution map of rainfall erosivity factors (K127–K139+800)

4.2.2 Soil erodibility factor (*K*)

The soil data of the slope in each section was obtained by sampling on the basis of the spatial distribution map of soil types in the study area and dividing the linear distribution of the soil. The calculation method of the *K* value was adopted by Sharply (Sharpley and Williams 1990) (Formula 4) to obtain the soil erodibility factor values of each slope, as shown in Tables 3 and 4.

$$K = 0.2 + 0.3e^{[0.0256SAN(1-SIL/100)]} \times \left(\frac{SIL}{CLA+SIL} \right)^{0.3} \times \left[1 - \frac{0.25C}{C + e^{3.72-2.95C}} \right] \times \left[1 - \frac{0.75N_1}{SN_1 + e^{22.9SN_1-5.51}} \right] \quad (4)$$

In the formula, SAN, SIL, CLA, and C represent sand grains (0.05–2 mm), powder (0.002–0.05 mm), clay (<0.002 mm), and organic carbon content (%), $SN_1=1-SAN/100$, respectively.

Table 3. Soil data for natural slope catchment areas

A section of a expressway	Sand (%)	Silt (%)	Clay (%)	Organic carbon (%)	<i>K</i>
K83+500–K84+900	51.50	33.00	15.50	0.75	0.3064
K85+200–K85+300	67.00	24.00	9.00	2.1	0.2546
K85+500–K86	75.40	18.90	5.70	0.83	0.2483
K86+300–K87+600	71.00	19.70	9.30	1.12	0.2522
K88+200–K90+200	66.80	20.00	13.20	1.18	0.2561
K90+200–K92+700	70.00	15.20	14.80	1.73	0.2397
K93–K94	33.30	29.00	37.70	1.05	0.3161



K94~K95	42.60	34.00	23.40	0.74	0.3205
K96+900~K97+800	58.00	25.00	17.00	2.7	0.2630
K97+800~K99	65.00	23.00	12.00	2.8	0.2541
K99~K100+500	60.00	12.00	28.00	1.15	0.2476
K100+500~K101+100	60.00	16.00	24.00	0.95	0.2580
K101+100~K102+100	71.00	9.90	19.10	0.73	0.2384
K102+100~K104	70.00	12.30	17.70	1.72	0.2355
K104~K105	66.00	20.50	13.50	0.79	0.2630
K105~K106+910	60.00	26.50	13.50	1.05	0.2775
K106+910~K109+100	61.00	15.00	24.00	1.18	0.2521
K109+100~K110+100	58.00	12.80	29.20	1.28	0.2490
K110+100~K111+100	61.50	14.00	24.50	1.33	0.2479
K111+100~K112+100	59.00	13.20	27.80	1.57	0.2458
K112+500~K113+500	63.00	18.10	18.90	1.66	0.2503
K114+900~K115+900	69.00	17.50	13.50	1.88	0.2434
K115+900~K116+800	55.90	24.20	19.90	1.06	0.2766
K117~K118	59.00	13.30	27.70	1.4	0.2477
K118~K121	58.00	13.00	29.00	1.58	0.2461
K121~K122	60.40	11.20	28.40	1.05	0.2470
K122~K123	57.00	14.20	28.80	1.02	0.2562
K123~K125	58.10	12.90	29.00	1.37	0.2480
K125~K126	62.40	12.80	24.80	1.42	0.2440
K126~K129	63.30	14.70	22.00	1.57	0.2452
K129~K131	59.00	13.10	27.90	1.08	0.2515
K131~K134+300	62.00	13.30	24.70	1.24	0.2473
K134+500~K135+800	59.00	13.80	27.20	1.28	0.2501
K136~K137	59.00	13.60	27.40	1.33	0.2491
K137~K138	61.00	13.20	25.80	1.53	0.2447
K138~K139	65.10	13.40	21.50	1.16	0.2461

Table 4. Soil data for artificial slope catchment areas

A section of a expressway	Sand (%)	Silt (%)	Clay (%)	Organic carbon (%)	<i>K</i>
K83+500~K84+900	40.10	33.00	26.90	0.75	0.3216
K85+200~K86	74.00	18.00	8.00	0.78	0.2491
K86+300~K87+600	72.00	19.00	9.00	0.83	0.2531
K88+200~K89+400	64.90	20.90	14.20	1.01	0.2622
K89+600~K90+600	60.00	23.10	16.90	0.86	0.2735
K90+600~K91+600	47.60	35.00	17.40	0.725	0.3164
K91+600~K92+600	31.10	29.00	39.90	0.96	0.3222
K92+900~K94+200	32.60	36.60	30.80	0.74	0.3421
K96+900~K97+800	29.00	50.00	21.00	0.92	0.3746
K97+800~K99	42.30	49.00	8.70	0.91	0.3544
K99~K100+500	37.00	50.20	12.80	0.75	0.3686
K100+500~K101+100	41.50	52.00	6.50	0.95	0.3619



K101+100~K102+100	41.00	42.50	16.50	0.73	0.3438
K102+100~K104	40.70	27.00	32.30	1.02	0.3015
K104~K105	50.00	27.80	22.20	0.79	0.2956
K105~K106+910	46.00	37.80	16.20	1.05	0.3179
K106+910~K109+100	51.00	32.00	17.00	1.18	0.2955
K109+100~K110+100	58.00	22.00	20.00	1.02	0.2708
K110+100~K111+100	57.40	25.10	17.50	1.03	0.2775
K111+100~K112+100	43.00	31.00	26.00	1.07	0.3058
K112+500~K113+500	30.60	29.70	39.70	0.76	0.3291
K114+900~K115+900	31.90	27.50	40.60	0.89	0.3192
K115+900~K116+800	35.40	24.20	40.40	1.06	0.3020
K117~K118	57.00	14.00	29.00	0.94	0.2568
K118~K121	59.80	13.00	27.20	1.03	0.2513
K121~K122	54.00	22.10	23.90	1.05	0.2745
K122~K123	57.00	24.70	18.30	1.02	0.2773
K123~K125	49.00	22.20	28.80	0.93	0.2823
K125~K126	52.50	20.40	27.10	0.88	0.2753
K126~K129	53.50	24.60	21.90	0.91	0.2827
K129~K131	49.50	23.30	27.20	1.08	0.2812
K131~K134+300	42.00	25.50	32.50	1.04	0.2960
K134+500~K135+800	49.00	33.80	17.20	1.02	0.3059
K136~K137	32.00	33.00	35.00	1.03	0.3275
K137~K138	28.00	22.00	50.00	1.05	0.3094
K138~K139	50.00	27.00	23.00	1.06	0.2888
K139~K139+800	38.50	33.40	28.10	1.09	0.3167

4.2.3 Calculation of topographic factors in natural slope catchments

(1) Slope length factor

According to the topographic map and highway design of Xinhe Expressway with 1:2000 scale, the slope length and factor of slope catchment were calculated using DEM data with 0.5 m spatial resolution generated by ArcGIS. The natural slope catchment slope was divided into less than 1°, 1°–3°, 3°–5°, and greater than or equal to 5° using the Reclassify tool in ArcGIS. The operation formula adopted the L factor algorithm proposed by Moore and Burch (Moore and Burch 1986), as shown by Formulas (5) and (6).

$$L = \left(\frac{\lambda}{22.13} \right)^m \quad (5)$$

$$\lambda = \text{flowacc} \cdot \text{cellsize} \quad (6)$$

In the formula, L is normalized to the amount of soil erosion along the slope length of 22.13 m, λ is the slope length, flowacc is the total pixel number of water flowing into the pixel that is higher than the pixel, and cellsize refers to the DEM resolution size. The value is 0.5 m, and m is the LS factor. See Formula (7).



$$m = \begin{cases} 0.2 & \theta < 1^\circ \\ 0.3 & 1^\circ \leq \theta < 3^\circ \\ 0.4 & 3^\circ \leq \theta < 5^\circ \\ 0.5 & \theta \geq 5^\circ \end{cases}, \quad (7)$$

where θ is the slope.

(2) Slope factor

The S factor was calculated as follows. If the slope is less than 18° , then the formula proposed by McCool et al (Mccol et al., 1987) was used. If the slope was greater than 18° , then the formula proposed by Baoyuan Liu was adopted (Liu et al., 1994), See Formula (8).

$$S = \begin{cases} 10.8 \cdot \sin \theta + 0.03 & \theta < 9^\circ \\ 16.8 \cdot \sin \theta - 0.05 & 9^\circ \leq \theta < 18^\circ \\ 21.9 \cdot \sin \theta - 0.96 & \theta \geq 18^\circ \end{cases} \quad (8)$$

The DEM data were processed by ArcGIS, thus obtaining slope data. The slope values of each prediction unit were extracted using the Zonal statistics tool. Through the classification tool in ArcGIS, the slope of the highway slope catchment of Xinhe was divided into less than 9° , 9° – 18° , and greater than or equal to 18° .

The S values of the slope catchments under the three slope grade conditions were calculated by combining Formula (8) and ArcGIS techniques. The LS values of the slope prediction units are shown in Figure 8.

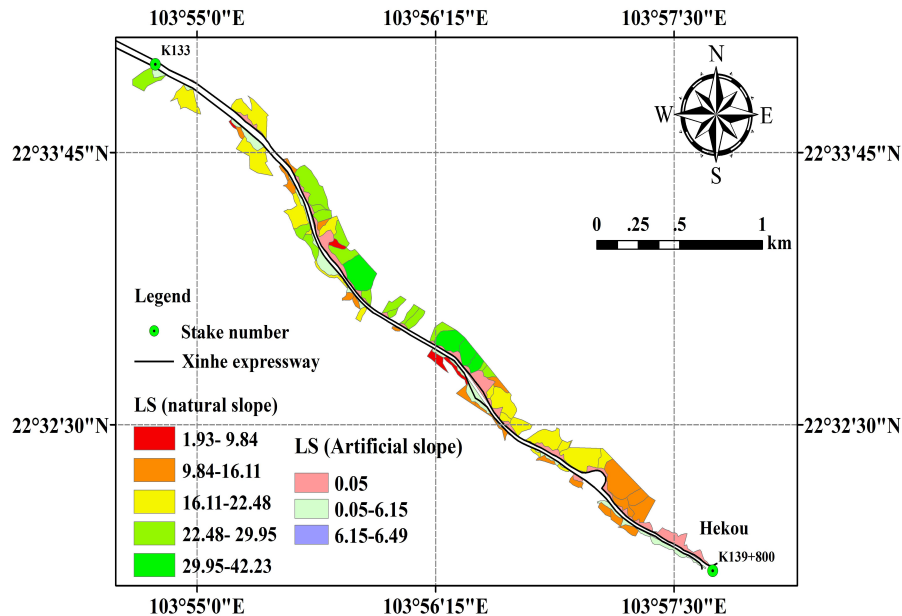


Figure 8. Spatial distribution map of topographic factors (K134–K139)



4.2.4 Calculation of topographic factors of artificial slopes

(1) Slope length factor

The method of Zongwei Chen (2010) was used to calculate the LS factor of the artificial slopes (Chen et al., 2010), and the calculation method for the topographic factors of the artificial slopes of Xinhe Expressway was modified. The slope length factor (L_a) was calculated using Formulas (5) and (6). The slope length index (m_a) was measured by runoff plot experiment and then calculated by Formula (9).

$$m_a = \log_{\frac{\lambda_1}{\lambda_2}} \frac{A_1}{A_2}, \quad (9)$$

where A_1 and A_2 are the soil erosion intensity values of two slopes when the slope lengths are λ_1 and λ_2 , respectively. The specifications of the two slopes are the same except for slope length. The soil erosion amounts under 30 erosion rainfall conditions were monitored in the runoff field of Xiao Xinzhai of Mengzi City in 2014–2015 (Table 5). The m_a value under each rainfall condition was calculated using Formula (9) according to the monitoring value of soil erosion amount. The average value of m_a is 0.32, which is the m_a value of artificial slope length factor, as shown in Table 6.

Table 5. Amount of soil erosion of monitoring areas ($t \cdot km^{-2}$)

The time of the second rainfall	1	2	3	4	5	6
2014.06.05	4212	5158	5922	6423	12896	888
2014.06.07	1997	2447	2812	3089	6170	426
2014.06.17	867	1098	1227	1341	2664	185
2014.06.28	5700	7128	8107	8979	17915	1225
2014.07.01	477	608	686	748	1498	103
2014.07.13	1560	1915	2159	2374	4757	327
2014.07.20	3857	4878	5617	6183	12323	849
2014.08.02	5601	7048	7939	8600	17231	1194
2014.08.12	1955	2491	2881	3148	6294	435
2014.08.26	6211	7630	8750	9561	19196	1315
2014.08.29	1539	1889	2161	2356	4701	326
2014.09.02	611	758	868	950	1910	131
2014.09.04	1487	1893	2172	2372	4761	324
2014.09.17	1577	1954	2250	2451	4809	336
2014.09.20	1076	1329	1512	1633	3252	224
2014.10.05	749	925	1064	1172	2356	160
2015.07.04	5216	6377	7260	7877	15653	1090
2015.07.15	1575	1925	2192	2416	4775	334
2015.07.24	991	1250	1394	1522	3002	212
2015.07.28	4200	5188	5907	6544	13005	886
2015.08.13	829	1057	1189	1292	2567	177
2015.08.19	1010	1233	1390	1521	3016	208
2015.08.26	1682	2108	2415	2673	5263	364
2015.09.03	386	481	543	583	1169	81



2015.09.12	591	745	857	940	1868	129
2015.09.17	1172	1433	1632	1789	3555	245
2015.09.25	1369	1690	1906	2089	4152	287
2015.10.03	1188	1468	1671	1832	3664	252
2015.10.08	2908	3707	4220	4599	9196	625
2015.10.12	779	963	1111	1215	2339	164

Table 6. Calculation results of m_a

The time of the second rainfall	m_{12}	m_{13}	m_{14}	m_{23}	m_{24}	m_{34}
2014.06.05	0.29	0.31	0.30	0.34	0.32	0.28
2014.06.07	0.29	0.31	0.31	0.34	0.34	0.33
2014.06.17	0.34	0.32	0.31	0.27	0.29	0.31
2014.06.28	0.32	0.32	0.33	0.32	0.33	0.36
2014.07.01	0.35	0.33	0.32	0.30	0.30	0.30
2014.07.13	0.30	0.30	0.30	0.30	0.31	0.33
2014.07.20	0.34	0.34	0.34	0.35	0.34	0.34
2014.08.02	0.33	0.32	0.31	0.29	0.29	0.28
2014.08.12	0.35	0.35	0.34	0.36	0.34	0.31
2014.08.26	0.30	0.31	0.31	0.34	0.33	0.31
2014.08.29	0.30	0.31	0.31	0.33	0.32	0.30
2014.09.02	0.31	0.32	0.32	0.34	0.33	0.32
2014.09.04	0.35	0.35	0.34	0.34	0.33	0.31
2014.09.17	0.31	0.32	0.32	0.35	0.33	0.30
2014.09.20	0.30	0.31	0.30	0.32	0.30	0.27
2014.10.05	0.30	0.32	0.32	0.35	0.34	0.34
2015.07.04	0.29	0.30	0.30	0.32	0.30	0.29
2015.07.15	0.29	0.30	0.31	0.32	0.33	0.34
2015.07.24	0.33	0.31	0.31	0.27	0.28	0.31
2015.07.28	0.31	0.31	0.32	0.32	0.33	0.36
2015.08.13	0.35	0.33	0.32	0.29	0.29	0.29
2015.08.19	0.29	0.29	0.30	0.30	0.30	0.32
2015.08.26	0.33	0.33	0.33	0.34	0.34	0.36
2015.09.03	0.32	0.31	0.30	0.30	0.28	0.25
2015.09.12	0.34	0.34	0.34	0.35	0.34	0.32
2015.09.17	0.29	0.30	0.30	0.32	0.32	0.32
2015.09.25	0.30	0.30	0.30	0.30	0.31	0.32
2015.10.03	0.31	0.31	0.31	0.32	0.32	0.32
2015.10.08	0.35	0.34	0.33	0.32	0.31	0.30
2015.10.12	0.31	0.32	0.32	0.35	0.33	0.31
The average value of m_a	0.32					

(2) Slope factor

The calculation of slope factor was based on the research method of Zongwei Chen (Chen et al., 2010). Six runoff plots were set up in the Xiao xinzhai runoff field of Mengzi City. The soil



erosion intensity under slope conditions of 1:1.5, 1:1.0, and 9:100 was monitored. Then, the slope factor under the slope condition was obtained using Formula (10).

$$S_{\theta} = \frac{A_{\theta}}{A}, \quad (10)$$

where S_{θ} represents the slope factor when the slope is θ , A_{θ} represents the soil erosion intensity when the slope is θ (t/hm^2), and A represents the soil erosion intensity when the slope is 9% (t/hm^2). The three slope conditions (1:1.5, 1:1.0, and control slope 9:100) in the soil erosion monitoring experiment, combined with Formula (10), were used to calculate the slope factor values of the two kinds of slopes (1:1.5 and 1:1.0) under the 30 rainfall conditions. The average factors of the slopes under the 1:1.5 and 1:1.0 slope conditions are 7.28 and 14.49, respectively (Table 7).

After the slope design drawings were digitized by ArcGIS, the slope and length values of each artificial slope prediction unit were determined according to the design specifications. The slope length value of each artificial slope prediction unit was the horizontal projection length of the cement frame. The slope length of six aris brick revetment was 0. Formulas (5), (6), (9), and (10), combined with the slope length factor and m_a and S_{θ} values, were used to calculate the value of LS of each artificial slope prediction unit.

Table 7. Calculation results of slope factor

The time of the second rainfall	$S_{1.5}$	$S_{1.0}$
2014.06.05	7.23	14.52
2014.06.07	7.25	14.47
2014.06.17	7.25	14.41
2014.06.28	7.33	14.62
2014.07.01	7.28	14.57
2014.07.13	7.27	14.57
2014.07.20	7.28	14.52
2014.08.02	7.20	14.43
2014.08.12	7.23	14.46
2014.08.26	7.27	14.60
2014.08.29	7.24	14.44
2014.09.02	7.25	14.56
2014.09.04	7.33	14.72
2014.09.17	7.30	14.32
2014.09.20	7.28	14.49
2014.10.05	7.33	14.73
2015.07.04	7.23	14.36
2015.07.15	7.24	14.32
2015.07.24	7.17	14.15
2015.07.28	7.39	14.68
2015.08.13	7.28	14.47
2015.08.19	7.33	14.53
2015.08.26	7.35	14.47



2015.09.03	7.22	14.47
2015.09.12	7.28	14.47
2015.09.17	7.29	14.48
2015.09.25	7.28	14.47
2015.10.03	7.27	14.53
2015.10.08	7.36	14.71
2015.10.12	7.40	14.26
Average	7.28	14.49

Note: S_y represents the slope factor value simultaneously solved by erosion intensity values for monitoring plots numbered x and y .

4.2.5 Cover and management practice factor

The C factor reflects the effect of vegetation cover and management on soil erosion (Yoder et al., 1993). Good correlation was observed between management factors and vegetation coverage. Therefore, the NDVI was used to calculate the vegetation coverage. Then, the C factor was estimated (Feng and Zhao 2014), as shown in Formula (11). Then, the vegetation coverage data were corrected by selecting a sample plot every 2 km along the study area for investigation. Finally, accurate vegetation coverage data were obtained (Figure 9). The C factor map of the soil erosion prediction unit in the slope catchment area is shown in Figure 10.

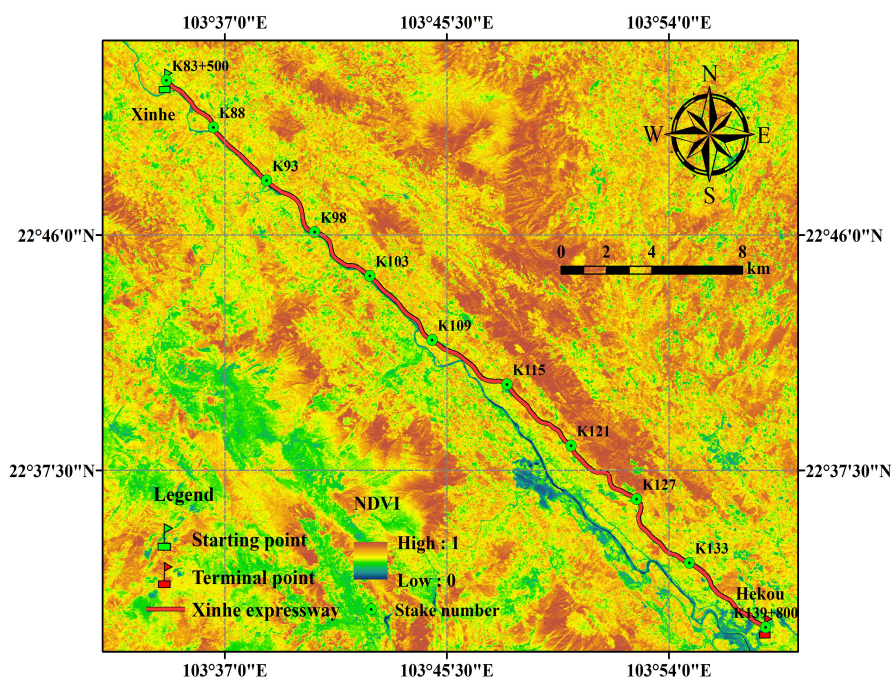


Figure 9. Vegetation coverage along Xinhe Expressway

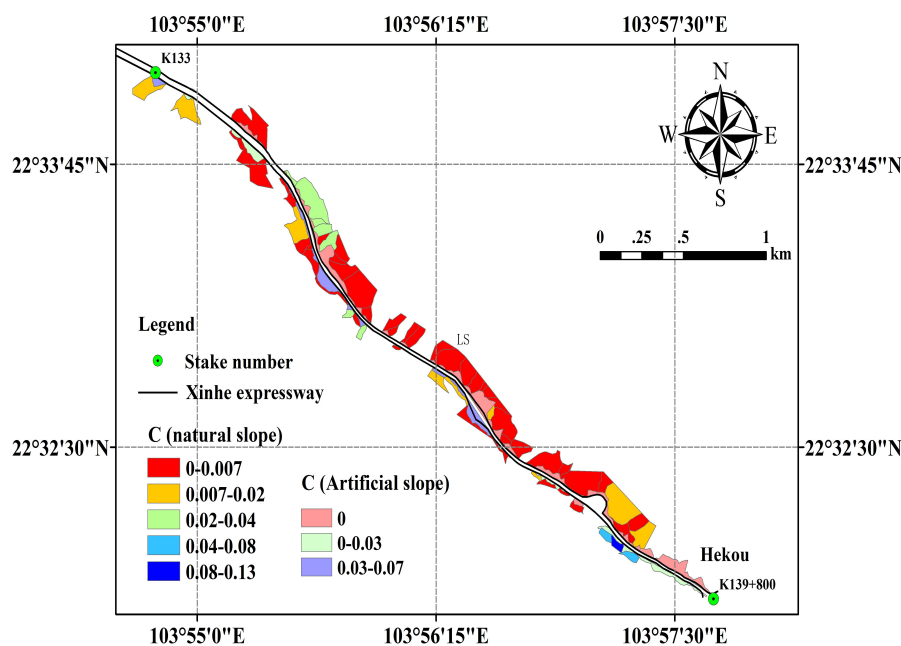


Figure 10. Spatial distribution map of cover and management practice factor

4.2.6 Factor of soil and water conservation measures

The land use types of the natural slope catchment area were mainly cultivated, forest, construction, and difficult lands. Through field investigation and visual judgment, the water conservation measures of the farmland and forestland were identified to be mainly contour belt tillage, horizontal terrace and terrace, and artificial slope catchment area, including cement frame and six arris brick revetments. The *P* values of the cement frame and the six arris brick revetment were determined by the area ratio method as 0.85 and 0.4, respectively. The *P* values of the soil and water conservation measures are shown in Table 8.

Table 8. *P* values of different slope types

Slope type	Cement frame	Hexagonal brick	Contour strip tillage	Level bench/Terrace	Construction land	Difficult to use land	Other
<i>P</i>	0.85	0.4	0.55	0.03	0	0.2	1

4.3 Validation of model simulation accuracy

In this study, the monitoring of soil erosion in three monitoring areas under 16 erosive rainfall conditions was conducted in 2014. No rainfall occurred in the 24 h preceding each rainfall, and the disturbance of antecedent rainfall on soil erosion on the slopes was excluded. By estimating the historical soil and water loss of each slope prediction unit, the results were compared with data



from three monitoring plots along the side slope of Xinha Expressway, as shown in Table 9.

Table 9. Comparison of model prediction and monitoring results

The time of the second rainfall	K83+550		K93+550		K133+550	
	Monitoring (t·km ⁻²)	Analog (t·km ⁻²)	Monitoring (t·km ⁻²)	Analog (t·km ⁻²)	Monitoring (t·km ⁻²)	Analog (t·km ⁻²)
2014.06.05	305.56	219.70	397.25	287.21	115.61	83.24
2014.06.07	86.36	118.96	93.86	131.71	29.32	39.95
2014.06.17	102.72	141.10	44.50	62.43	12.75	17.32
2014.06.28	276.73	197.31	507.44	367.04	159.33	113.12
2014.07.01	22.74	16.44	39.62	28.68	13.50	9.82
2014.07.13	138.70	98.89	154.29	108.28	42.86	30.61
2014.07.20	538.04	392.77	325.12	235.19	108.57	77.34
2014.08.02	206.14	292.40	137.01	192.02	83.22	113.38
2014.08.12	125.18	168.03	132.33	185.85	28.76	39.95
2014.08.26	197.98	269.35	298.75	418.76	89.17	123.25
2014.08.29	60.84	83.00	80.03	113.95	22.51	30.61
2014.09.02	83.17	61.38	87.15	62.13	16.32	11.91
2014.09.04	119.24	87.76	96.53	131.38	40.59	29.88
2014.09.17	119.08	85.98	96.61	133.50	42.12	31.17
2014.09.20	24.62	33.82	40.79	57.23	15.41	21.26
2014.10.05	31.18	22.70	28.51	39.98	11.03	14.99

The error analysis shows that under the 16 rainfall conditions, the absolute errors of the three monitoring areas were 47.15, 52.52, and 16.27 t·km⁻² and the overall average absolute error was 38.65 t·km⁻². The average relative errors were 31.80%, 35.49%, and 32.26%, and the overall mean relative error was 31.18%. The root mean square errors were 59.44, 65.64, and 20.95, all of which were within the acceptable range. The Nash efficiency coefficient of the model was 0.67, which was between 0 and 1 and thus shows that the model accuracy satisfied the requirements. The calculation results are shown in Tables 10–12.

Table 10. Statistical table of absolute error (t·km⁻²)

The time of the second rainfall	K83+550	K93+550	K133+550
2014.06.05	85.86	110.04	32.37
2014.06.07	32.59	37.85	10.63
2014.06.17	38.38	17.94	4.57
2014.06.28	79.42	140.40	46.20
2014.07.01	6.30	10.94	3.68
2014.07.13	39.81	46.01	12.25
2014.07.20	145.27	89.93	31.24



2014.08.02	86.26	55.01	30.16
2014.08.12	42.85	53.53	11.19
2014.08.26	71.38	120.01	34.08
2014.08.29	22.16	33.92	8.10
2014.09.02	21.79	25.02	4.41
2014.09.04	31.48	34.86	10.71
2014.09.17	33.10	36.89	10.95
2014.09.20	9.20	16.44	5.85
2014.10.05	8.48	11.48	3.96
Average	47.15	52.52	16.27

Table 11. Statistical table of relative error (%)

The time of the second rainfall	K83+550	K93+550	K133+550
2014.06.05	28.10%	27.70%	28.00%
2014.06.07	37.74%	40.33%	36.24%
2014.06.17	37.36%	40.31%	35.87%
2014.06.28	28.70%	27.67%	29.00%
2014.07.01	27.70%	27.61%	27.23%
2014.07.13	28.70%	29.82%	28.59%
2014.07.20	27.00%	27.66%	28.77%
2014.08.02	41.84%	40.15%	36.24%
2014.08.12	34.23%	40.45%	38.89%
2014.08.26	36.05%	40.17%	38.22%
2014.08.29	36.43%	42.38%	35.98%
2014.09.02	26.20%	28.71%	27.00%
2014.09.04	26.40%	36.11%	26.39%
2014.09.17	27.80%	38.18%	26.00%
2014.09.20	37.36%	40.29%	37.93%
2014.10.05	27.20%	40.27%	35.87%
Average	31.80%	35.49%	32.26%

Table 12. Statistical table of root mean square error

A section of a expressway	Natural slope catchment area		
	K83+550	K93+550	K133+550
RMSE	59.44	65.64	20.95

The analysis accuracy revealed that the northern and flat terrain of the southern region had a small simulation error due to the high and low areas of the central region of the terrain, which resulted in a slightly lower accuracy than that of the southern region. Under heavy rainfall



conditions, the absolute error value of the simulation was large. On the one hand, the result may be caused by the artificial error in monitoring the sediment collection in the area. On the other hand, the model itself may be defective.

4.4 Application of early warning of soil erosion to mountain expressway

The rainfall data and I_{50} values in the 20 years covered by the study were obtained from the meteorological departments of Mengzi, Pingbian, Jinping, and Hekou counties in Yunnan Province. Rainfall and rainfall intensity were interpolated using cokriging, which was introduced into elevation and geographical position, as shown in Figures 11 and 12.

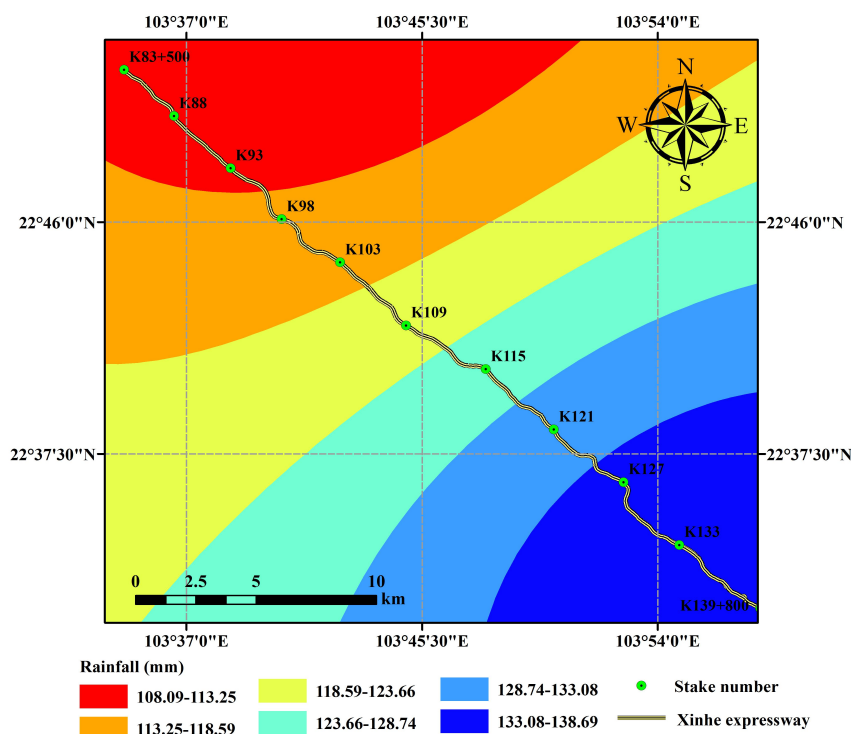


Figure 11. Rainfall interpolation results under 20-year return

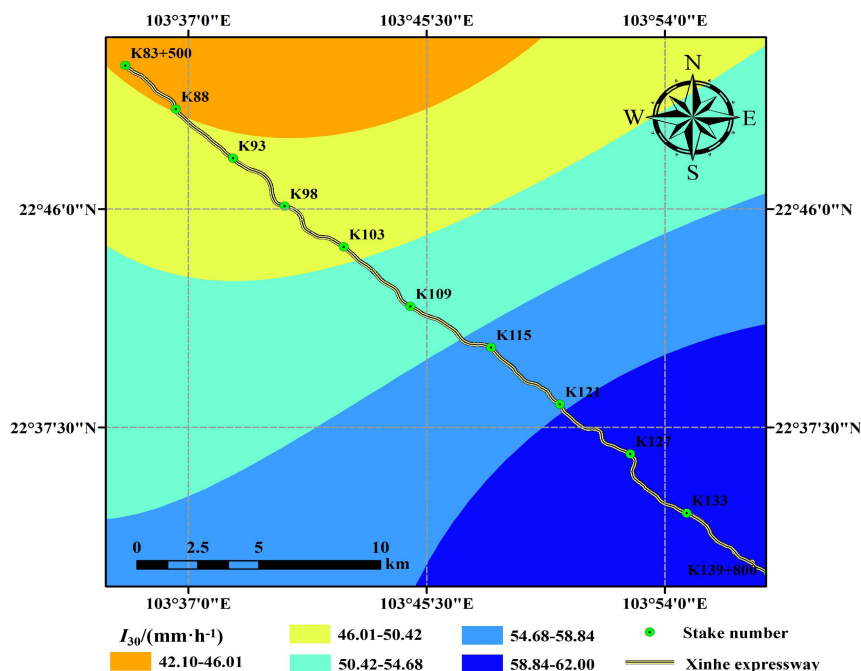


Figure 12. Rainfall intensity interpolation results under 20-year return

The total soil erosion amount of each prediction unit using 20-year rainfall data was obtained by simulation according to the soil erosion intensity classification standard. The prediction results were classified as “no risk,” “slight risk,” “moderate risk,” “high risk,” and “extremely high risk,” (Yuan 1999) as shown in Figure 13.

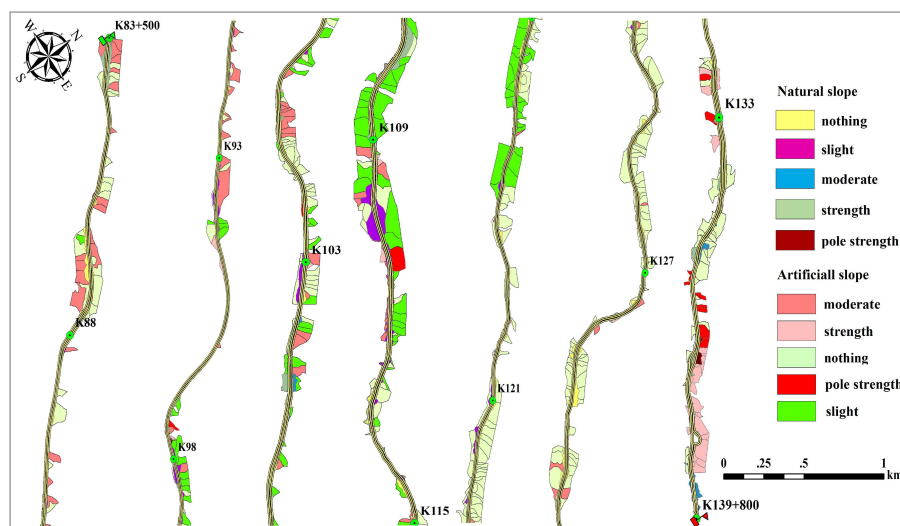


Figure 13. Risk analysis of soil and water loss under 20-year rainfall conditions



The grading results showed that the percentage of prediction units classified under risk-free and mild risk for soil and water loss was 88.60%. The risk of soil erosion was low in these areas. Thus, road traffic safety was not affected. The percentage of prediction units that were classified under moderate risk was 4.29%. The risk of soil erosion in these areas was relatively low under the general rainfall intensity. However, under high rainfall intensity, a certain scale of soil erosion disaster could occur. The percentage of prediction units that were labeled high and extremely high risk was 7.11%. The risk of soil erosion was great in these units. For example, from K134+500 to K135+500 (1000 m), the average soil erosion amount on both sides of the slope under 20-year rainfall amount was up to 1757 t/km². Even if only a portion of the sediment was deposited on the road, road safety would be affected.

Similarly, the risk of soil erosion was analyzed according to the grading standard of risk of soil and water loss under the condition of 20 year rainfall by simulating the soil erosion amount of each prediction unit under one-year rainfall amount (Figure 14).

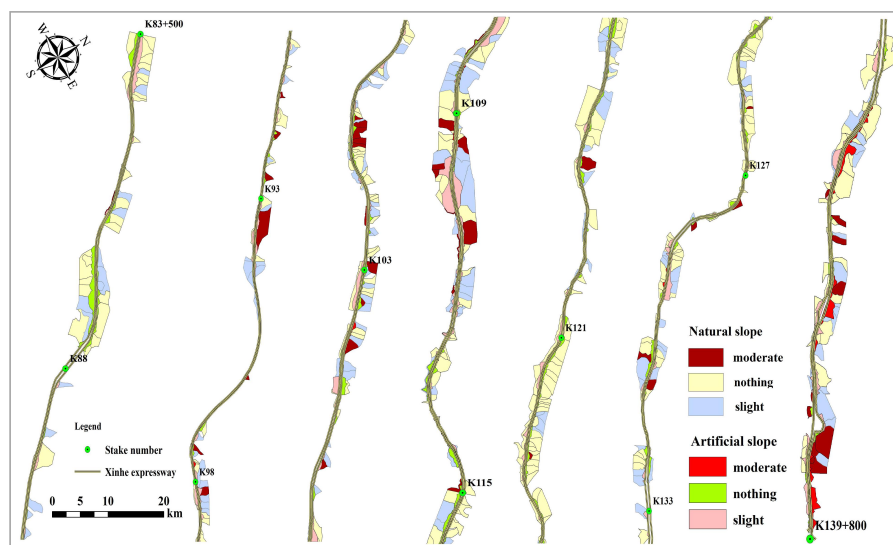


Figure 14. Risk analysis of soil and water loss under one-year rainfall amount

The results indicated that the percentages of prediction units at no and mild soil erosion risks were 78.00% and 17.92%, respectively. The risk of soil erosion was low in these areas. Thus, the safety of road traffic would not be affected. The percentage of prediction units at risk of mild soil erosion was 6.08%. The layout of soil and water conservation measures in these areas should therefore be rationally adjusted. Moreover, the comprehensive management of their slopes should be strengthened, and plant and engineering measures should be applied comprehensively to complete the work of soil and water conservation in these regions. Inspections should be reinforced and motorists should be reminded to pay attention to traffic safety during the rainy



season. Most of the artificial slopes covered by the study are made of six arris brick revetment, the amount of soil erosion is small, but the frame-type cement slope protection against soil erosion is sturdier than that in other areas. Slope protection measures should be rationally adjusted according to predicted results. A cement box should be added in the soil a year before the beginning of the rainy season to prevent soil erosion caused by slope scouring, which affects the road stability and traffic safety.

5 Conclusions

- (1) This study fully considered the differences between the model parameters of the artificial and natural slopes of mountain expressways. Each catchment area was considered a unit. The artificial and natural slope prediction units were then divided, thus producing 422 artificial slope prediction units and 814 natural slope catchment prediction units. The soil and water loss of each slope was predicted in real time, thus making the prediction of soil erosion accurate.
- (2) The R factor used the space interpolation method and the P factor of the artificial slope was corrected by the area ratio method in determining the parameters of model prediction. The other factors were corrected by the experimental data.
- (3) Error analysis of the actual observation data revealed that the overall average absolute error of each monitoring area was $38.65 \text{ t}\cdot\text{km}^{-2}$, the average relative error was 31.18%, the root mean square error was between 20.95 and 65.64, and the Nash efficiency coefficient was 0.67. The method of soil and water loss prediction adopted in this paper generally has less error and higher prediction accuracy than other models and can satisfy prediction requirements.
- (4) The risk grades of soil and water loss along the slope of Xinhe Expressway were divided into 20- and one-year rainfall on the basis of the simulated prediction. The results showed that the percentage of slope area with high and extremely high risk was 7.11%, which was observed mainly in K109+500–K110+500 and K133–K139+800 sections. Therefore, relevant departments should strengthen disaster prevention and reduction efforts, as well as corresponding water and soil conservation initiatives, in these areas.

6 Acknowledgements

This research work was supported jointly by the Yunnan Provincial Communications Department Project [2012-272-(1)] and the Yunnan Provincial Science and Technology Commission Project (2014RA074).

7 References

- Angulomartínez, M., and Beguería, S.: Estimating rainfall erosivity from daily precipitation records: a comparison among methods using data from the ebro basin (NE Spain). *Journal of Hydrology*, 379(1): 111-121, 2009.



- Chen, B. H.: The study on multivariate spatial interpolation method of precipitation in mountainous areas. Beijing Forestry University, 2016 (in Chinese).
- Chen, F., Zeng, M. G., and Zhou, Z. H.: Evaluation for Ecological Benefits of Greening on Expressways in Mountainous Area. *Technology of Highway and Transport*, 1:139-143, 2015 (in Chinese).
- Chen, Y. J., Sun, K. M., and Zhao, Y.: Experiment on the effect of rule caused by slope angle on sand and runoff under the condition of ecological protected slope. *Journal of Water Resources & Water Engineering*, 21(4):55-59, 2010 (in Chinese).
- Chen, Z. W., He, F., and Wang, J. J.: Revises of Terrain Factors of Roadbed Side Slope in Universal Soil Loss Equation. *HIGHWAY*, 12:180-185, 2010 (in Chinese).
- Feng, Q., and Zhao, W. W.: The study on cover-management factor in USLE and RUSLE: a review. *ACTA ECOLOGICA SINICA*, 34(16):4461-4472, 2014 (in Chinese).
- Fenta, A. A., Yasuda, H., Shimizu, K., Haregeweyn, N., and Negussie, A.: Dynamics of Soil Erosion as Influenced by Watershed Management Practices: A Case Study of the Agula Watershed in the Semi-Arid Highlands of Northern Ethiopia. *Environmental Management*, 58(5): 1-17, 2016.
- Gong, J., and Yang, P.: Study on the Layout of Soil and Water Conservation Monitoring Sites during the Construction of Mountain Highways-Case Study of Enlai, Enqian Highway. *Subtropical Soil and Water Conservation*, 28(1):9-11, 2016 (in Chinese).
- Jia, Z. R., Guo, and Z. Y.: Quantifying Evaluation Approach to Highway Soil Bioengineering. *Research of Soil and Water Conservation*, 15(2):260-262, 2008 (in Chinese).
- Jiang, M., Pan, X. Y., Nie, W. T.: Preliminary analysis of prevention and control of soil and water loss in expressway project construction. *Yangtze River*, 48(12):61-64, 2017 (in Chinese).
- Kinnell, P. I. A.: Applying the RUSLE and the USLE-M on hillslopes where runoff production during an erosion event is spatially variable. *Journal of Hydrology*, 519:3328-3337, 2014.
- Lin, H. L., Zheng, S. T., and Wang, X. L.: Soil erosion assessment based on the RUSLE model in the Three-Rivers Headwaters area, Qinghai-Tibetan Plateau, China. *ACTA PRATACULTURAE SINICA*, 26(7):11-22, 2017 (in Chinese)
- Liu, B. Y., Nearing, M. A., Shi, P. J., and Jia, Z. W.: Slope length effects on soil loss for steep slopes. *Soil Science Society of America Journal* 64(5): 1759-1763, 2000.
- Liu, X. Y.: Study on the slope stability and its rheological influence in Mountain highway. Central South University, 2013.
- Mccool, D. K., Brown, L. C., Foster, G. R., Mutchler, C. K., and Meyer, L. D.: Revised slope steepness factor for the universal soil loss equation. *Transactions of the ASAE-American Society of Agricultural Engineers (USA)*, 30(5): 1387-1396, 1987.
- Millward, A. A., and Mersey, J. E.: Adapting the rusle to model soil erosion potential in a mountainous tropical watershed. *Catena* 38(2):109-129, 1999.
- Molla, T., and Sisheber, B.: Estimating soil erosion risk and evaluating erosion control measures for soil conservation planning at Koga watershed in the highlands of Ethiopia. *Solid Earth*, 8, 1-23, 2017
- Moore, I. D., and Burch, G. J.: Physical basis of the length-slope factor in the universal soil loss equation. *Soil Science Society of America Journal*, 50(5): 1294-1298, 1986.
- Stanchi, S., Freppaz, M., Ceaglio, E., Maggioni, M., Meusburger, K., & Alewell, C., and Zanini, E.: Soil erosion in an avalanche release site (Valle d'Aosta: Italy): towards a winter factor for RUSLE in the Alps. *Natural Hazards & Earth System Sciences*, 14(7), 255-440, 2014.
- Panos, P., Cristiano, B., Pasquale, B., Katrin, M., Andreas, K., Svetla, R., Melita, P. T., Silas, M., Michaela, H., Preben, O., Juha, A., Mónica, L., Anna, R., Alexandru, D., Santiago, B., and Christine, A.: Rainfall erosivity in Europe. *Science of the Total Environment*, 511: 801, 2015.
- Renard, K. G., Foster, G. R., Weesies, G. A., Mccool, D. K., and Yoder, D. C.: Predicting soil erosion by water: a guide to conservation planning with the revised universal soil loss



- equation (RUSLE). Agriculture Handbook, 1997.
- Rick, D., Van, R., Matthew, E. H., and Robert J. H.: Estimating the LS Factor for RUSLE through Iterative Slope Length Processing of Digital Elevation Data within ArcInfo Grid. *Cartography*, 30(1): 27-35, 2001.
- Bosco, C., De Rigo, D., Dewitte, O., Poesen, J., and Panagos, P.: Modelling soil erosion at european scale: towards harmonization and reproducibility. *Natural Hazards & Earth System Sciences*, 2(4), 2639-2680, 2015.
- Shamshad, A., Azhari, M. N., Isa, M. H., Hussin, W. M. A. W., and Parida, B. P.: Development of an appropriate procedure for estimation of RUSLE EI_{30} index and preparation of erosivity maps for Pulau Penang in Peninsular Malaysia. *Catena*, 72(3): 423-432, 2008.
- Sharpley, A. N., and Williams, J. R.: EPIC-erosion/productivity impact calculator: 2. User manual. Technical Bulletin-United States Department of Agriculture, 4(4): 206-207, 1990.
- Shi, Z. H., Cai, C. F., Ding, S. W., Wang, T. W., and Chow, T. L.: Soil conservation planning at the small watershed level using RUSLE with GIS: a case study in the three gorge area of china. *Catena*, 55(1): 33-48, 2004.
- Silburn, D. M.: Hillslope runoff and erosion on duplex soils in grazing lands in semi-arid central Queensland. III. USLE erodibility (K factors) and cover-soil loss relationships. *Soil Research*, 49(49): 127-134, 2011.
- Song, F. L., Ma, Y. H., Zhang, C. X., Yu, H. M., Hu, H. X., He, J. L., and Huang, J. Y.: Research progress on greening substrate material of ecological protection of expressway-side slope. *Science of Soil and Water Conservation*, 6:57-61, 2008 (in Chinese).
- Tan, S. H., and Wang, Y. M.: Research Progress and Thinking of Bioengineering Techniques for Slope Protection in Expressway. *Research of Soil and Water Conservation*, 11(3):81-84, 2004 (in Chinese).
- Tresch, S., Meusbürger, K., and Alewell, C.: Influence of slope steepness on soil erosion modelling with RUSLE, measured with rainfall simulations on subalpine slopes. *Bulletin of Hokkaido Prefectural Agricultural Experiment Stations*, 1995.
- Wang, H. J., Yang, Y., and Wang, W. J.: Prediction of Soil Loss Quantity on Side Slope of Freeway Construction: Amendments to Main Parameters of USLE. *Journal of Wuhan University of Technology (Transportation Science & Engineering)*, 29(1):12-15, 2005.
- Wang, K., and Gao, Z. L.: Analysis of Bioengineering Technology for Slope Protection of Expressway: Taking Expressway from Ankang to the Border of Shaanxi and Hubei as an Example. *Ecological Economy*, 31(5):155-159, 2015 (in Chinese).
- Wang, L. H., Ma, B., and Wu, F. Q.: Effects of wheat stubble on runoff, infiltration, and erosion of farmland on the Loess Plateau, China, subjected to simulated rainfall. *Solid Earth*, 8(2), 1-28, 2017.
- Wang, W. Z., and Jiao, J. Y.: Quantitative Evaluation on Factors Influencing Soil Erosion in China. *Bulletin of Soil and Water Conservation*, (st):1-20, 1996 (in Chinese).
- Wang, W. Z., and Zhang, X. K.: Distribution of Rainfall Erosivity R Value in China. *Journal of soil erosion and soil conservation*, 2(1): 7-18, 1995.
- Wischmeier, W. H., and Smith, D. D.: Predicting rainfall-erosion losses from cropland east of the rocky mountains: a guide to conservation planning, 1965.
- Xiao, P. Q., Shi, X. J., Chen, J. N., Wu, Q., Yang, J. F., Yang, C. X., and Wang, C. G.: Experimental Study on Protecting Speedway Slope Under Rainfall and Flow Scouring. *Bulletin of Soil and Water Conservation*, 24(1):16-18, 2004 (in Chinese).
- Yang, X.: Deriving rusle cover factor from time-series fractional vegetation cover for hillslope erosion modelling in new south wales. *Soil Research*, 52(52): 253-261, 2014.
- Yang, Y. C., Wang, M. Z., Xu, Y. Y., Wang, P. C., and Song, Z. P.: Prediction of Soil Erosion on Embankment Slope of Qinhuangdao-Shenyang Special Line for Passenger Trains. *Journal of Soil and Water Conservation*, 15(2):14-16, 2001(in Chinese).



- Yang, Y., and Wang, K.: Discussions on the Side Slope Protection System For Expressway. *Industrial Safety and Environmental Protection*, 32(1):47-49, 2006 (in Chinese).
- Yoder, D. C., Foster, G. R., Renard, K. G., Weesies, G. A., and Mccool, D. K.: C-factor calculations in RUSLE. American Society of Agricultural Engineers. Meeting (USA), 1993.
- Yuan, J. P.: Preliminary Study on Grade Scale of Soil Erosion Intensity. *Bulletin of Soil and Water Conservation*, 19(6):54-57, 1999 (in Chinese).
- Zeng, C., Wang, S. J., Bai, X. Y., Li, Y. B., Tian, Y. C., Li, Y., Wu, L. H., and Luo, G. J. : Soil erosion evolution and spatial correlation analysis in a typical karst geomorphology using RUSLE with GIS. *Solid Earth*, 8(4), 1-26, 2017.
- Zhou, F. C.: Highway Slope Ecological Protection Against Erosion Mechanism and Control Effect Research. Chongqing jiaotong university, 2010 (in Chinese).
- Zhu, S. Q., Lin, J. L., and Lin, W. L.: Preliminary Study on Effects of Expressway Construction on Side-Slope Soil Erosion in Mountainous Areas. *Resources Science*, 26(1):54-60, 2004 (in Chinese).
- Zhuo, M. N., Li, D. Q., and Zheng, Y. J.: Study on Soil and Water Conservation Effect of Bioengineering Techniques for Slope Protection in Highway. *Journal of Soil and Water Conservation*, 20(1):164-167, 2006 (in Chinese).